Supplemental Material for: Quantum Zeno blockade in optomechanical systems

Karl Pelka[1] and André Xuereb[1]

[1]*Department of Physics, University of Malta, Msida MSD 2080, Malta*

(Dated: September 10, 2025)

I. FORMATION OF ZENO SUBSPACES IN BOSONIC SYSTEMS

In order to understand the formation of the Zeno subspaces that evolve independent of each other, we discuss the consequences of the strong coupling mechanism [1] for the bosonic modes. We note that a time dependent change of basis commutes with the determination of the Zeno Hamiltonian in Eq. (2) of the main text, if the unitary $\hat{U}(t)$ that describes the basis change commutes with all projectors $[\hat{U}(t), \hat{P}_j] = 0$. To apply this theorem to our system, we assume that the coupling operator $\hat{O}$ commutes with the projector onto any number state $\hat{P}_{nm} = (|n\rangle \otimes |m\rangle)(\langle n| \otimes \langle m|)$ which allows us to go into the frame rotating with the optical frequency ω_L and mechanical frequency Ω_D. This is described by the unitary transformation $\hat{U}(t) = \exp(-i(\omega_L \hat{a}^\dagger \hat{a} + \Omega_D \hat{b}^\dagger \hat{b})t)$ and we find the Zeno Hamiltonian

$$\hat{H}_Z/\hbar = \Delta \hat{a}^\dagger \hat{a} + \delta \hat{b}^\dagger \hat{b} + g\hat{O} + \sum_k \hat{P}_k \hat{H}_o \hat{P}_k. \tag{1}$$

The projected Hamiltonian of the system under observation now depends on the spectrum of the measurement Hamiltonian. In absence of any coupling $\hat{O}$, the frequency spectrum is given in terms of the quantum numbers n, m as $\omega_{n,m} = \Delta n + \delta m$ and we find that the detuning parameters determine the occuring degeneracies. In the case that both detunings vanish, the spectrum is fully degenerate and the single projector $\hat{P}_1$ onto the eigenvalue 0 is the identity operator on the entire Hilbert space $\mathbb{1}_{\mathcal{H}}$ which leads to the Zeno Hamiltonian

$$\hat{H}_Z = \hat{P}_1 \hat{H}_o \hat{P}_1 = \hat{H}_o = i\hbar E(\hat{a}^\dagger - \hat{a}) + i\hbar D(\hat{b}^\dagger - \hat{b}). \tag{2}$$

This results in the Zeno evolution $\mathcal{U}_Z(t) = \hat{D}_a(iEt)\hat{D}_b(iDt)$ with the displacement operators $\hat{D}_a(\alpha) = \exp(\alpha^* \hat{a} - \alpha \hat{a}^\dagger)$ and $\hat{D}_b(\beta) = \exp(\beta^* \hat{b} - \beta \hat{b}^\dagger)$. In the case that only one detuning is vanishing, say $\Delta = 0$, we find that there exist countably many subspaces enumerated with the eigenvalue $\eta_m = \delta m$ with the corresponding projector $P_m = \mathbb{1}_a \otimes (|m\rangle \langle m|)$. We find the Zeno Hamiltonian $\hat{H}_Z/\hbar = \delta \hat{b}^\dagger \hat{b} + iE(\hat{a}^\dagger - \hat{a})$ which shows the partition of the Hilbert space $\mathcal{H}$ into subspaces $\mathcal{H}_m$ that are evolving independently. The evolution of any pure state $|\Psi(0)\rangle = |\psi_a(0)\rangle \otimes (\sum_m c_m |m\rangle)$, for instance, is given by $|\Psi(t)\rangle = \hat{D}_a(iEt)\,|\psi_a(0)\rangle \otimes (\sum_m c_m e^{im\delta t}\,|m\rangle)$. Likewise, the case where the mechanical detuning is vanishing leads to

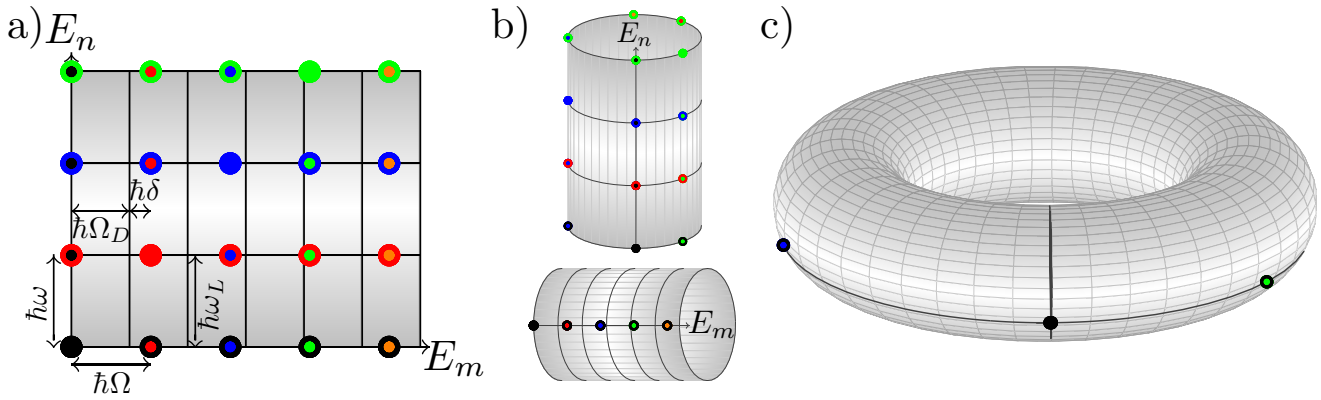

FIG. 1. (Color online) Visualization of the formation of invariant quantum Zeno subspaces for driven bosonic modes. a) The energy eigenvalues for two bosonic modes can be arranged in a two dimensional plane and the energy can be determined through the sum of the two coordinates. b) The behaviour of the drive Hamiltonian continuously observed through the bosonic modes can be determined by rolling up the energy eigenvalue plane with respect to the frequencies of both drives. If the drive frequency does not match the frequency spacing as shown in the upper diagram, the energy eigenvalues sweep the cylinder and hence the drive does not allow transitions among the corresponding states. If the energy eigenvalues coalesce as in the lower case, the states can be accessed through the drive. c) The drive generates invariant quantum Zeno subspaces and the dynamics within each subspace are given by the corresponding Zeno Hamiltonian.

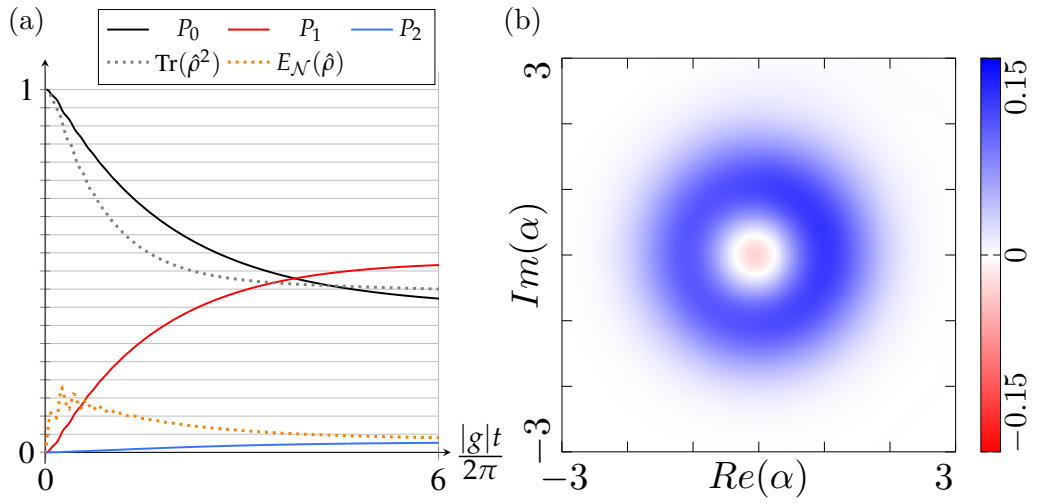

FIG. 2. (Color online) Quantum Zeno effect in an optomechanical cavity with an additional dispersive shift with strength $g_0 = 0.025|g|$ displaying a phonon blockade. (a) (solid) Probabilities to occupy zero (black), one (red), and two phonons (blue). (dashed) Additional charactarization of the quantum state through purity (gray) and logarithmic negativity (orange) (b) Resulting Wigner function of the final state.

a Hamiltonian that evolves independently in the subspaces with a given photon number and acts as a displacement operator $\hat{D}_b(iDt)$ in each of the subspaces. If neither detuning is vanishing (and they are not multiples of each other), all eigenvalues are distinct and the projection takes place over all projectors $\hat{P}_{nm} = (|n\rangle \otimes |m\rangle)(\langle n| \otimes \langle m|)$ which results in the vanishing of the dynamics $\sum_{n,m} \hat{P}_{nm}\hat{H}_o\hat{P}_{nm} = 0_{\mathcal{H}}$ of the system under observation. This analysis recovers the physical intuition behind the drive Hamiltonian $\hat{H}_o(t)$ that it acts as a displacement of the initial state with an amplitude increasing in time if and only if the respective drive is resonant. We find that the formation of the invariant subspaces can be understood with a geometrical construction depicted in Fig. 1: Instead of arranging the energy eigenvalues onto a one dimensional line (E_{nm}), it is possible to arrange the eigenvalues onto a two-dimensional plane (E_n, E_m) such that the total energy is given as the sum of the cartesian coordinates $E_{nm} = E_n + E_m$ as shown in Fig. 1(a). The behaviour of the drive Hamiltonian $\hat{H}_o$ continuously observed through the bosonic modes $\hat{H}_c$ is determined by wrapping up the energy eigenvalue plane periodically with respect to the frequencies of both drives ω_L and Ω_D which is depicted in Fig. 1(b). As the drive frequency Ω_D does not match the frequency spacing Ω as shown in the upper diagram, the energy eigenvalues sweep the cylinder and hence the drive does not allow transitions among the corresponding states. States can only be accessed through the drive if the energy eigenvalues coalesce through this wrapping process as shown in the lower diagram. The complete analysis of the invariant quantum Zeno subspaces is shown in Fig. 1(c) and requires to wrap up the plane along both directions which results in the energy eigenvalues distributed on a torus. Invariant Zeno subspaces are determined by the coalescence of the energy eigenvalues and the dynamics within each subspace are given by the corresponding Zeno Hamiltonian.

II. FORMATION OF ZENO SUBSPACES IN NON-DIAGONAL HAMILTONIANS

As optomechanical experiments [2, 3] may contain dispersive interactions $\hat{H}_{\mathrm{OM}} = g_0\hat{a}^\dagger\hat{a}(\hat{b}^\dagger + \hat{b})$ in the Hamiltonian we inspect their effect on the quantum Zeno blockade if these non-diagonal terms cannot be eliminated. Assuming a non-diagonal measurement Hamiltonian $\hat{H}'_c$, there exists a unitary $\hat{V}$ that diagonalizes the self-adjoint Hamiltonian as $\hat{H}_c = \hat{V}\hat{H}'_c\hat{V}^\dagger$. Computing the Zeno Hamiltonian of the non-diagonal Hamiltonian [1] proceeds according to Eq. (2) in the main text with $\hat{H}'_Z = \hat{H}'_c + \sum_k \hat{P}'_k\hat{H}'_o\hat{P}'_k$, where $\hat{P}'_k$ are projectors onto the eigenspaces of $\hat{H}'_c$. A projection onto the eigenspaces of $\hat{H}'_c$ means that $\hat{P}_k = \hat{V}\hat{P}'_k\hat{V}^\dagger$ is the sum of projectors onto orthonormal basis vectors $|j\rangle$ that span the respective eigenspaces $\hat{P}_k = \sum_j |j\rangle\langle j|$. Therefore changing the basis of the Zeno Hamiltonian $\hat{H}_Z = \hat{V}\hat{H}'_Z\hat{V}^\dagger$ results in $\hat{H}_Z = \hat{V}\hat{H}'_c\hat{V}^\dagger + \sum_k \hat{V}\hat{P}'_k\hat{H}'_o\hat{P}'_k\hat{V}^\dagger$. By the unitary relation $\hat{V}\hat{V}^\dagger = \mathbb{1}$ and by inverting the relation of the projectors above $\hat{P}'_k = \hat{V}^\dagger\hat{P}_k\hat{V}$ and we find

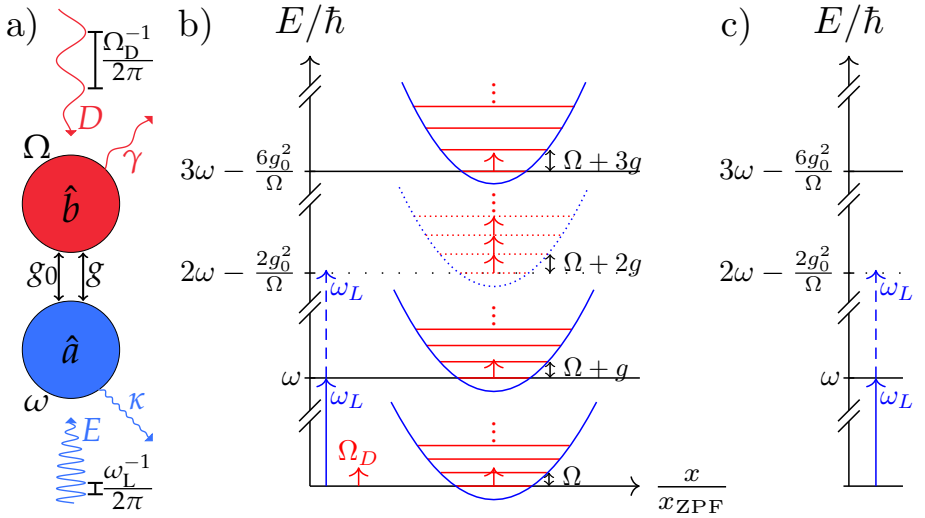

FIG. 3. (Color online) Quantum Zeno effect in an optomechanical cavity with dispersive shift. (a) An optomechanical system consisting of a mechanical and an optical mode both driven at distinct frequencies coupled through two nonlinearities. (b) A cross-Kerr nonlinearity enables a mechanical drive to address mechanical transitions solely for a particular photon number. The resonant states of the mechanical drive form a Zeno subspace which makes them inaccessible from the rest of the states. (c) The photonic spectrum experiences an anharmonicity but still lacks the state with the photon number tunable via the mechanical drive frequency and hence a photon blockade occurs independently of the self-Kerr shift of frequency $n(n-1)g_0^2/\Omega$.

$$\begin{aligned}\hat{H}_Z =& \hat{H}_c + \sum_k \hat{V}(\hat{V}^\dagger \hat{P}_k \hat{V})\hat{H}_o'(\hat{V}^\dagger \hat{P}_k \hat{V})\hat{V}^\dagger \\ =& \hat{H}_c + \sum_k (\hat{V}\hat{V}^\dagger)\hat{P}_k(\hat{V}\hat{H}_o'\hat{V}^\dagger)\hat{P}_k(\hat{V}\hat{V}^\dagger) \\ =& \hat{H}_c + \sum_k \hat{P}_k \hat{H}_o \hat{P}_k. \end{aligned} \tag{3}$$

This result implies that the quantum Zeno dynamics are basis independent but take a particularly simple form in a diagonal basis of $\hat{H}_c'$. To highlight this result, we use it to extend our analysis to our system in Eq. (1) in the main text that additionally interacts with a standard optomechanical Hamiltonian $\hat{H}_{\mathrm{OM}} = \hbar g_0 \hat{a}^\dagger \hat{a}(\hat{b}^\dagger + \hat{b})$.

In order to analyze the phonon blockade based on the quantum Zeno effect with a dispersive interaction, firstly the measurement Hamiltonian needs to be chosen as $\hat{H}_c/\hbar = \omega \hat{a}^\dagger \hat{a} + \Omega \hat{b}^\dagger \hat{b} + g\hat{a}^\dagger \hat{a}\hat{b}^\dagger \hat{b}$ and the observed Hamiltonian has to be chosen as $\hat{H}_o/\hbar = g_0 \hat{a}^\dagger \hat{a}(\hat{b}^\dagger + \hat{b}) - iE(\hat{a}^\dagger e^{-i\omega_L t} - \hat{a}e^{i\omega_L t}) - iD(\hat{b}^\dagger e^{-i\Omega_D t} - \hat{b}e^{i\Omega_D t})$. Then, the relevant basis change is a change $U_1 = \exp(-i\Omega_D \hat{b}^\dagger \hat{b} t)$ into the rotating frame of the mechanical oscillator in combination with a change $U_2 = \exp(-i\omega_L \hat{a}^\dagger \hat{a} t)$ into the rotating frame of the optical oscillator. Note that both operators clearly commute $V = U_1 U_2 = U_2 U_1$ and no complexity arises due to this choice of basis as the transformed measurement Hamiltonian is $\hat{H}_c'/\hbar = (\omega - \omega_L)\hat{a}^\dagger \hat{a} + (\Omega - \Omega_D)\hat{b}^\dagger \hat{b} + g\hat{a}^\dagger \hat{a}\hat{b}^\dagger \hat{b}$. The relevant spectrum of projectors onto the eigenspaces hence becomes $\omega_{nm} = (\omega - \omega_L + gm)n + (\Omega - \Omega_D)m$. If the optical drive frequency, which is a tunable parameter, is set as $\omega_L = \omega + Mg$ and $\Omega_D = \Omega$ then the spectrum turns into $\tilde{\omega}_{nm} = g(m - M)n$ which still possesses the degeneracy for $m = M$. Note that this derivation for the dispersive optomechanical shift $\hat{H}_{\mathrm{OM}} = \hbar g_0 \hat{a}^\dagger \hat{a}(\hat{b}^\dagger + \hat{b})$ does not employ any property of this interaction other than its relative weakness, and our argument is therefore equally valid for any arbitrary, but weak, interaction $\hbar \tilde{g}\hat{O}(\hat{a}, \hat{b})$, such that $|\tilde{g}| \ll |g|$.

In order to demonstrate the persistence of the Zeno phonon blockade in spite of an additional, symmetry-breaking dispersive shift, we conducted a numerical simulation of the system parameters in Fig. 4 of the main text with an additional dispersive shift, characterized by $g_0 = 0.025|g|$, resulting in Fig. 2. We see that the additional dispersive interaction does not impact the probabilities to occupy one or two phonon, the logarithmic negativity, and the Wigner function. The only impact is in the slower decay of the state's purity.

The photon blockade based on the quantum Zeno effect with dispersive interaction is analyzed by choosing the measurement Hamiltonian as $\hat{H}_c/\hbar = \Omega \hat{b}^\dagger \hat{b} + g_0 \hat{a}^\dagger \hat{a}(\hat{b}^\dagger + \hat{b}) + g\hat{a}^\dagger \hat{a}\hat{b}^\dagger \hat{b}$ and the observed Hamiltonian as $\hat{H}_o/\hbar = \omega \hat{a}^\dagger \hat{a} - iE(\hat{a}^\dagger e^{-i\omega_L t} - \hat{a}e^{i\omega_L t}) - iD(\hat{b}^\dagger e^{-i\Omega_D t} - \hat{b}e^{i\Omega_D t})$. The required basis change V in this case is the polaron transform given in [4] as $\hat{U}_3 =$

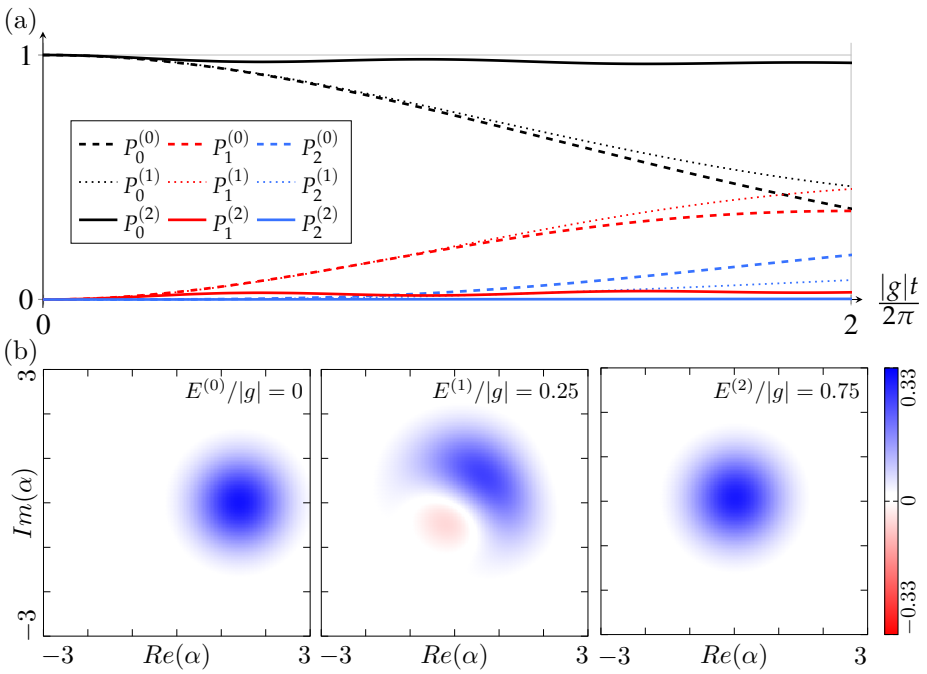

FIG. 4. (Color online) Analysis of resulting state from the quantum Zeno dynamics for the open system driven with $D^{(2)}/|g| = 0.065$ at frequency $\Omega_D = \Omega$. a) Probability to find zero (black), one (red), and two (blue) phonons in the mechanical subsystem over time for optical drive with $E^{(0)}/|g| = 0$ (dashed), $E^{(1)}/|g| = 0.25$ (dotted), and $E^{(2)}/|g| = 0.75$ (solid) at frequency $\omega_L = \omega + 2g + 4\chi$ and. b) Resulting Wigner function for $E^{(0)}/|g| = 0$ in the left panel showing a displacment of the mechanical state, $E^{(1)}/|g| = 0.25$ in the middle panel showing the occurrence of negative patches indicating the non-Gaussian state, and $E^{(2)}/|g| = 0.75$ disabling the displacement of the mechanical state.

$\exp((g_0/\Omega)\hat{a}^\dagger\hat{a}(\hat{b}^\dagger - \hat{b}))$ followed by change into the rotating frame of the mechanical oscillator $U_1 = \exp(-i\Omega_D\hat{b}^\dagger\hat{b}t)$ which is non-commutative $V = U_1U_3 \neq U_3U_1$. Employing this unitary, we find the measurement Hamiltonian $\hat{H}_c'/\hbar = (\Omega - \Omega_D)\hat{b}^\dagger\hat{b} + (g_0^2/\Omega)\hat{a}^\dagger\hat{a}^\dagger\hat{a}\hat{a} + g\hat{a}^\dagger\hat{a}\hat{b}^\dagger\hat{b}$ and the relevant spectrum is $\omega_{nm} = (\Omega - \Omega_D)m + gnm + (g_0^2/\Omega)n(n-1)$. Choosing the freely tunable mechanical drive as $\Omega_D = \Omega + Ng$ the spectrum is $\tilde{\omega}_{nm} = g(n-N)m + (g_0^2/\Omega)n(n-1)$ and there is a degeneracy for all states $|n = N\rangle|m\rangle$ with arbitrary m. Therefore, the photon blockade based on the quantum Zeno effect is unaffected by the additional dispersive optomechanical coupling of arbitrary strength. Thus we would observe the identical behaviour of the N-th photonic level removed from the optical ladder which is not equidistant but contains an anharmonicity as illustrated in Fig. 3. Finally, applying the polaron transform to a basis vector $\hat{V}(|n\rangle \otimes |m\rangle) = |n\rangle \otimes \hat{D}_b(ng_0/\Omega)|m\rangle$ shows that the photonic basis remains invariant under the basis transformation. This reveals that the interpretation of the excitations of oscillator $\hat{a}$ as photons is identical in both bases.

III. ANALYSIS OF ADDITIONAL PERTURBING INTERACTIONS

As our optomechanical realization is based on the experiments discussed in [2], it is worth investigating that it may come with additional nonlinear interactions that would lead to a Hamiltonian as outlined in [5]

$$\frac{\hat{H}_P}{\hbar} = \omega\hat{a}^\dagger\hat{a} + \Omega\hat{b}^\dagger\hat{b} + g\hat{a}^\dagger\hat{a}\hat{b}^\dagger\hat{b} + \chi\hat{a}^\dagger\hat{a}(\hat{b}^\dagger\hat{b})^2. \tag{4}$$

We conduct the analysis of the quantum Zeno effect by designating $\hat{H}_P$ as the measurement Hamiltonian $\hat{H}_c$ and the system under observation is described by $\hat{H}_o(t)$. The resulting spectrum derived in the frame rotating with the drive frequencies ω_L and Ω_D is given by

$$\tilde{\omega}_{nm} = (\Omega - \Omega_D)m + (\omega - \omega_L + gm + \chi m^2)n. \tag{5}$$

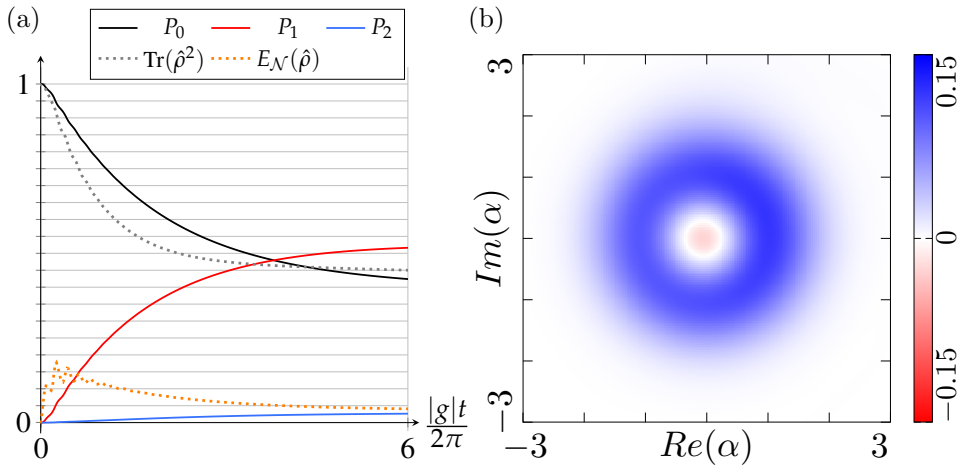

FIG. 5. (Color online) Analysis of resulting state from the quantum Zeno dynamics for the open system driven at $E^{(2)}/|g| = 0.75$ at frequency $\omega_L = \omega + g + \chi$ and $D^{(2)}/|g| = 0.065$ at frequency $\Omega_D = \Omega$. a) Probability to find zero (black), one (red), and two (blue) phonons in the mechanical subsystem over time showing a strong suppression of two or more phonons. b) Resulting Wigner function of the final state displaying a clear negative patch signalling the non-Gaussian nature of the state in the mechanical subsystem.

This spectrum shows that an optical drive tuned to $\omega_L = \omega + Mg + M^2\chi$ makes all states with M phonons degenerate. Hence, we find that in this optomechanical system the optical drive at frequency $\omega_L = \omega + Mg + M^2\chi$ removes the state with M phonons through the quantum Zeno effect from all remaining states.

We study the impact of the additional nonlinearity on the Zeno blockade by comparing the simulations outlined in the main text with the results for the same system but an additional nonlinearity characterised by $\chi/2\pi = 0.2$ MHz. Figure 4 shows the behaviour of an optical drive with amplitudes $E^{(0)}/|g| = 0$ (dashed), $E^{(1)}/|g| = 0.25$ (dotted), and $E^{(2)}/|g| = 0.75$ (solid) at a frequency of $\omega_L = \omega + 2g + 4\chi$ which establishes a blockade for two phonons. The results for a resonant mechanical drive at frequency $\Omega_D = \Omega$ with amplitude $D^{(2)}/|g| = 0.065$ strongly resemble Fig. 3 of the main text

and feature the negativity of the Wigner function at intermediate driving amplitude.

Similarly, Fig. 5 illustrates that the addition of the nonlinearity for the identical mechanical drive and an optical drive that establishes the blockade at for one phonon at frequency $\omega_L = \omega + g + \chi$ with amplitude $E^{(2)}/|g| = 0.75$ does not change the dynamics and Wigner function of the final state compared to the case without the perturbing nonlinearity displayed in Fig. 4 of the main text.

IV. MULTITONE STATE PREPARATION

The quantum Zeno blockade for intermediate couplings was found to suppress more than M excitations in the respective subsystem rather than remove the subspace with exactly M excitations which can be attributed to the non-adiabatic correction $\hat{U}_{\mathrm{na}}$ of the total evolution for finite coupling strengths [1]

$$\hat{U}_K(t) = \hat{U}_{\mathrm{ad},K}(t) + \frac{1}{K}\hat{U}_{\mathrm{na},K}(t), \tag{6}$$

where the non-adiabatic correction $\hat{U}_{\mathrm{na}}(t)$ is given by

$$\hat{U}_{\mathrm{na},K}(t) = \left[\sum_n \sum_{k\neq n} \frac{\hat{P}_k \hat{H}_o \hat{P}_n}{\eta_k - \eta_n}, \hat{U}_{\mathrm{ad},K}(t)\right] + \mathcal{O}(K^{-1}) \tag{7}$$

while the adiabatic evolution $\hat{U}_{\mathrm{ad},K}(t)$ is governed by

$$\hat{U}_{\mathrm{ad},K}(t) = \exp\left(-i\left(K\hat{H}_{\mathrm{m}} + \sum_n \hat{P}_n \hat{H}_o \hat{P}_n + K^{-1}\sum_n \sum_{k\neq n} \frac{\hat{P}_n \hat{H}_o \hat{P}_k \hat{H}_o \hat{P}_n}{\eta_n - \eta_k} + \mathcal{O}(K^{-2})\right)t\right). \tag{8}$$

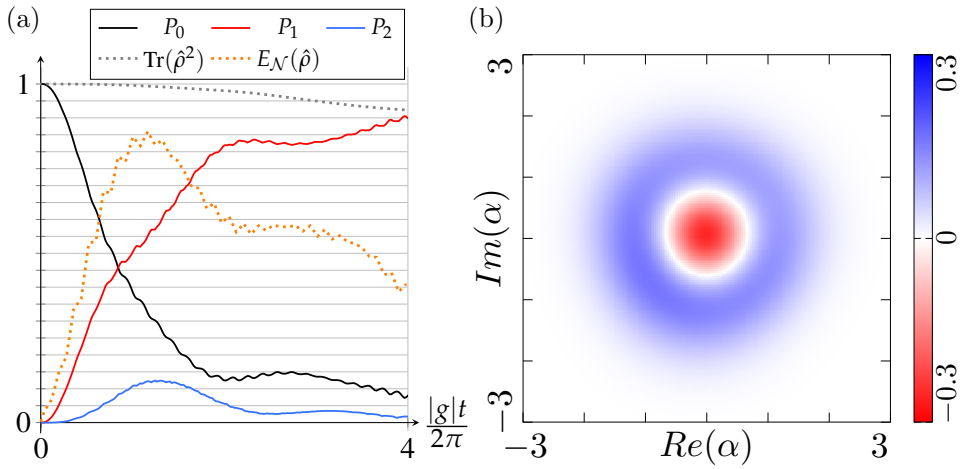

FIG. 6. (Color online) Analysis of resulting state from the quantum Zeno dynamics with multiple blocking tones in the open system with reduced optical decay. a) Probabilities for no phonon (black), one phonon (red), and two phonons (blue) over time. Characterisation of the quantum state through purity (gray, dashed) and logarithmic negativity (orange, dashed). b) Resulting Wigner function of the final state.

However, the simulations in the main text suggest that the transition from a state below M excitations into the subspace with M excitations is suppressed as well as the transition from M excitations to the subspace with $M+1$. Therefore, we find that the transitions from a state with fewer than M to a state with more than M excitations is suppressed twice and hence more effectively blocked. Thus, establishing multiple blockades that remove $M-1$ and M excitations in the strong coupling limit can improve the effective blockade for M excitations. Therefore, we employ the driving Hamiltonian

$$\hat{H}_o(t) = [i(E_1 e^{i\omega_1 t} + E_2 e^{i\omega_2 t})\hat{a} + i\tilde{D}e^{i\Omega_D t}\hat{b} + \text{h.c.}]. \tag{9}$$

with $\omega_1 = \omega + g + \chi$ and $\omega_2 = \omega + 2g + 4\chi$ to establish the combined blockade and $\Omega_D = \Omega$ to resonantly drive the mechanical subsystem. We employ $\tilde{\omega}/2\pi = \omega/2\pi = 5$ GHz and decay rate $\tilde{\kappa}/2\pi = 0.1 \times \kappa/2\pi = 6.48$ kHz for the optical mode while the mechanical mode, the coupling constants and mean occupations of the baths remain the same. Using the drive amplitude for the blockade $E_1/|g| = 0.075$ of the first level and $E_2/|g| = 0.497$ of the second level, as well as the drive amplitude of the mechanical system $\tilde{D}/|g| = 0.0497$ results in the dynamics for the probabilities and Wigner function illustrated in Fig. 6. In comparison to the blockade with a single drive tone, we find that the probability to find two phonons decays beyond the first Rabi-like oscillation towards an improved blockade at the final time $t_F = 8\pi/|g|$ with $1 - P_0 - P_1 = 0.0216$, as displayed in Fig. 6(a). Moreover, we find the probability of the Fock states $P_1(t_F) = 0.905$ and $P_2(t_F) = 0.018$. These results demonstrate that the suggested QZE scheme enables the creation of Fock states for systems which need to improve only the cavity linewidth by one order of magnitude beyond current state of the art. In addition, we find that the logarithmic negativity of the two-mode quantum state $\hat{\rho}$ initially assumes much larger values before it decays and the purity of the state decays much slower through the decrase of the optical decay rate. The corresponding Wigner function is presented in Fig. 6(b) which shows the similarity of the simulated state to the Fock state $|1\rangle$ as it consists of a large negative patch around the origin in phase space enclosed by a positive with an overall rotation symmetry.

[1] P. Facchi, *Quantum Zeno effect, Adiabacity and Dynamical Superselection Rules*, Fund. Aspects Quant. Phys. **17**, 197 (2011).

[2] T. T. Heikkilä, F. Massel, J. Tuorila, R. Khan, and M. A. Sillanpää, *Enhancing Optomechanical Coupling via the Josephson Effect*, Phys. Rev. Lett. **112**, 203603 (2014).

[3] T. T. Heikkilä, S. U. Cho, F. Massel, J. Tuorila, T. T. Heikkilä, P. J Hakonen, and M. A. Sillanpää, *Cavity optomechanics mediated by a quantum two-level system*, Nat. Comm. **6**, 6981 (2015).

[4] P. Rabl, *Photon Blockade Effect in Optomechanical Systems*, Phys. Rev. Lett. **107**, 063601 (2011).

[5] H. Solki, A. Motazedifard, and M. H. Naderi, *Improving photon blockade, entanglement, and mechanical-cat-state generation in a generalized cross-Kerr optomechanical circuit*, Phys. Rev. A **108**, 063505 (2023).